Thermophysical Properties and Pool Boiling Characteristics of Water-in-Polyalphaolefin Nanoemulsion Fluids

Jiajun Xu

Bao Yang[1]

Department of Mechanical Engineering,
University of Maryland,
College Park, MD 20742

Boualem Hammouda

Center for Neutron Research,
National Institute of Standards and Technology,
Gaithersburg, MD 20899

In this work, thermophysical properties, microstructure, and pool boiling characteristics of water-in-polyalphaolefin (PAO) nanoemulsion fluids have been measured in the water concentration range of 0–10.3 vol. %, in order to gain basic data for nanoemulsion boiling. Water-in-PAO nanoemulsion fluids are formed via self-assembly with surfactant: sodium sullfosuccinate (AOT). Thermal conductivity of these fluids is found to increase monotonically with water concentration, as expected from the Maxwell equation. Unlike thermal conductivity, their dynamic viscosity first increases with water concentration, reaches a maximum at 5.3 vol. %, and then decreases. The observed maximum viscosity could be attributed to the attractive forces among water droplets. The microstructures of the water-in-PAO nanoemulsion fluids are measured via the small-angle neutron scattering (SANS) technique, which shows a transition from sphere to elongated cylinder when the water concentration increases above 5.3 vol. %. The pool boiling heat transfer of these water-in-PAO nanoemulsion fluids is measured on a horizontal Pt wire at room temperature (25 °C, subcooled condition). One interesting phenomenon observed is that the pool boiling follows two different curves randomly when the water concentration is in the range of 5.3 vol. % to 7.8 vol. %. [DOI: 10.1115/1.4024423]

Keywords: nanoemulsion, pool boiling, thermophysical property, small-angle neutron scattering

1 Introduction

Cooling high heat flux electronics and optoelectronics are one of the most challenging problems in industry and military areas [1–34]. The coolants, lubricants, and other heat transfer fluids used in today's thermal systems typically have relatively poor heat transfer properties. Hence, heat transfer fluids with improved thermal properties are urgently needed. Recently, the authors had proposed a new "nanoemulsion heat transfer fluid" system in which one liquid is dispersed into another immiscible liquid as self-assembled nanodroplets to improve the fluid thermal properties [8–10,12,13]. The nanoemulsion heat transfer fluids belong to the family of microemulsion and are thermodynamically stable which is different from widely used emulsions [19–24,30,35–41]. The dispersed low boiling point fluid is expected to modify the thermophysical properties of base oil especially its phase change behavior.

In this study, thermophysical properties and pool boiling characteristics of water-in-PAO nanoemulsion fluids and their dependence on water concentration have been investigated experimentally. The microstructure of these fluids is also characterized via small-angle neutron scattering technique.

2 Experimental Apparatus and Procedure

2.1 Synthesis of Water-in-PAO Nanoemulsion Fluids. The water-in-PAO nanoemulsion fluids are spontaneously formed by self-assembly and are especially designed for enhanced heat transfer capability via addition of phase changeable fluids, such as water (as done here). These water nanodroplets are reverse micelles swollen with water, and stabilized by the surfactant AOT molecules (sigma Aldrich) that have hydrophilic heads facing inward and hydrophobic tails facing outward into the base fluid PAO (Chevron Philips Chemical Company).

The water-in-PAO nanoemulsion fluids are transparent, but scatter light due to the Tyndall effect [42,43], as shown in Fig. 1. Their microstructure and dynamics are highly dependent upon the molar ratio of water to AOT. Therefore, their thermophysical properties and pool boiling heat transfer characteristics are expected to vary with the molar ratio of water to AOT. In this study, 12 water-in-PAO nanoemulsion fluid samples with water

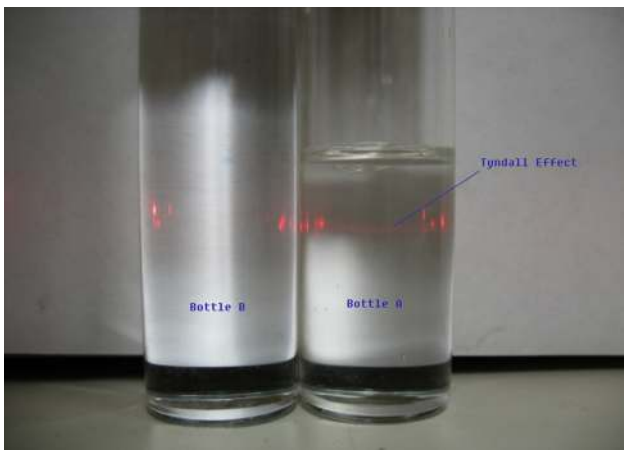

Fig. 1 Water-in-PAO nanoemulsion fluid (bottle A) and pure PAO (bottle B). The Tyndall effect can be seen in the nanoemulsion fluid (bottle A).

[1]Corresponding author.

Contributed by the Heat Transfer Division of ASME for publication in the JOURNAL OF HEAT TRANSFER. Manuscript received June 29, 2012; final manuscript received January 17, 2013; published online July 26, 2013. Guest Editors: G. P. "Bud" Peterson and Zhuomin Zhang.

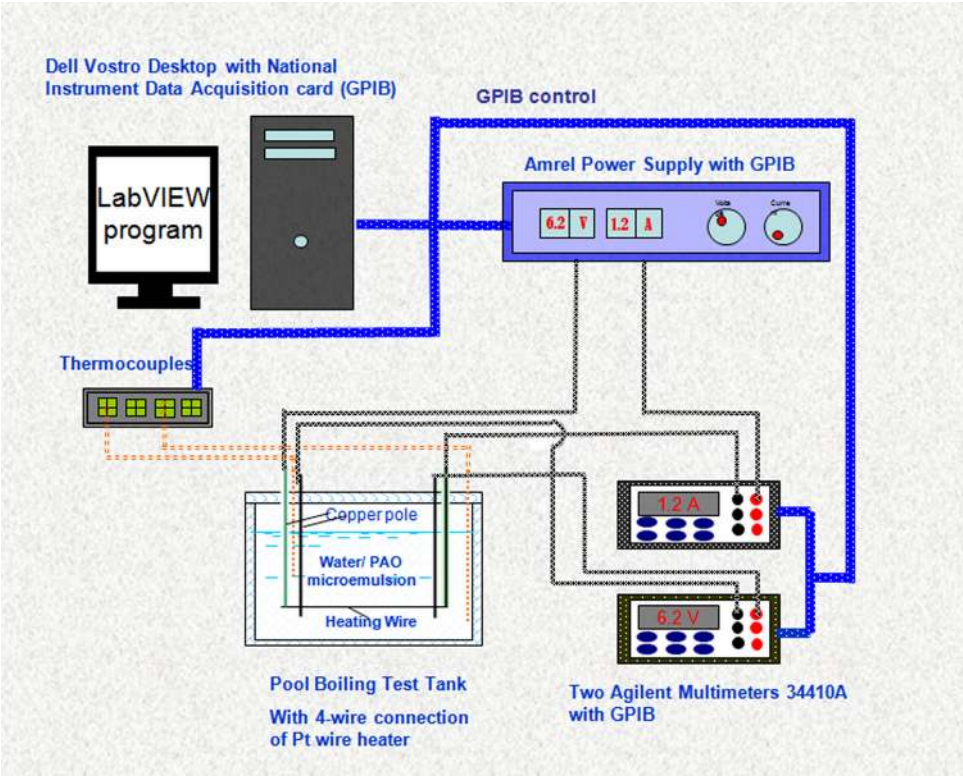

Fig. 2 Schematic of pool boiling test apparatus

volume fraction ϕ from 0.47% to 10.3%, equivalent to molar ratios from 0.8 to 19.2, are investigated.

2.2 Measurement of Thermal Conductivity and Viscosity. Thermal conductivity of the water-in-PAO nanoemulsion fluids is measured at room temperature using a 3ω-wire technique [8,10–14,44,45]. This technique is a combination of the hot-wire method and the 3ω method. In the measurement, a sinusoidal current at frequency ω is passed through the metal wire and then a heat wave at frequency 2ω is generated in the liquid. The 2ω temperature rise of the wire can be deduced by the voltage component at frequency 3ω. The thermal conductivity of the liquid, k, is determined by the slope of the 2ω temperature rise of the metal wire

$$k = \frac{p}{4\pi l} \cdot \left(\frac{\partial T_{2\omega}}{\partial In\omega} \right)^{-1} \tag{1}$$

where p is the applied electric power, ω the frequency of the applied electric current, l the length of the metal wire, and $T_{2\omega}$ the amplitude of temperature oscillation at frequency 2ω in the metal wire. Pure PAO is used for calibration and its measured value $k_{\mathrm{PAO}} = 0.14\ \mathrm{W}/(\mathrm{m} \cdot \mathrm{K})$ agrees well with the literature value [46].

The dynamic viscosity of the pure PAO and ethanol/PAO nanoemulsion fluids was measured using a commercial viscometer (Brookfield DV-I Prime).

2.3 SANS Measurement. The microstructure of water-in-PAO nanoemulsion fluid is measured via the SANS technique to detect the property-structure relation [35,40,47–55]. Unlike dynamic light scattering, SANS can be applied to "concentrated" colloidal suspensions (e.g., >1 vol. %) for the in situ determination of the particle size. In our SANS experiment, samples are prepared using deuterated alcohol to achieve the needed contrast between the droplets and the solvent. SANS measurements are conducted on the NG-3(30 m) beamline at the NIST Center for Neutron Research (NCNR) in Gaithersburg, MD. Samples are loaded into 2-mm quartz cells. The scattering intensity I is measured versus the scattering vector $q = 4\pi \sin(\theta/2)/\lambda$, where λ is the wavelength of the incident neutrons and θ is the scattering angle. The approximation $q = 2\pi\theta/\lambda$ is used for SANS (due to the small-angle θ).

2.4 Measurement of Pool Boiling Heat Transfer. Figure 2 shows the experimental apparatus for measurement of pool boiling heat transfer in water-in-PAO nanoemulsion fluids with different water concentrations. A platinum wire 25 μm in diameter is horizontally hanged in the test vessel, which serves as both the heater and thermometer. It is heated electrically via a dc power supply (ePower SPS150-8-20 V) and the voltage and current are recorded using multimeters (Agilent 34401 A and 34410 A). A transparent glass vessel is used to hold the liquids and allows visual observation. Ten milliliter sample is needed for each test. Such small amount is essential for screening a large number of samples in search for high performance thermal fluids. The test vessel is immersed in a water bath to maintain at a constant room temperature. Two K-type thermocouples are used to monitor temperatures, one for the sample and the other for water bath.

The experimental system is controlled by a LABVIEW program. The wall heat flux is calculated from the measured voltage and current directly. The wire temperature is determined from the relation between the electrical resistance and temperature of the platinum wire. Heat flux to the heated wire is stepwise increased till the wire burns out. The critical heat flux (CHF) is measured within an accuracy of 5%. Each sample is tested at least eight times to confirm that there is no deterioration of the fluid and the repeatability of the boiling curves. The uncertainty of measurement is listed in Table 1.

The SEM images of the Pt wires are obtained before and after boiling, and no surface modification is observed in the present experiment.

Table 1 Uncertainty of measurement

Measured quantity	Value and uncertainty: Range	Value and uncertainty: ± (% of reading + % of range)
$\Delta V_{\text{voltage sensor probes}}$	100.0 mV	0.0030 + 0.0030
	1.0 V	0.0020 + 0.006
	10 V	0.0015 + 0.0004
I_{current}	1.0 mA	0.007 + 0.006
	10.0 mA	0.007 + 0.02
	100.0 mA	0.010 + 0.004
	1.0 A	0.050 + 0.006
Temperature (type K)	−50 to 1382 °F	1 °F

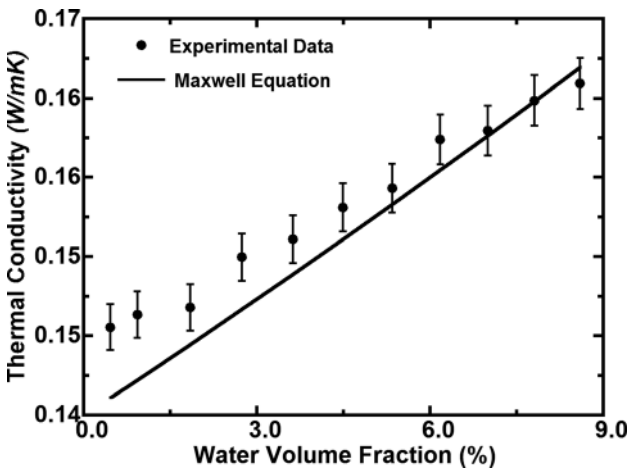

Fig. 3 Thermal conductivity of water-in-PAO nanoemulsion fluids versus water volume fraction. The prediction from the Maxwell equation is shown for comparison.

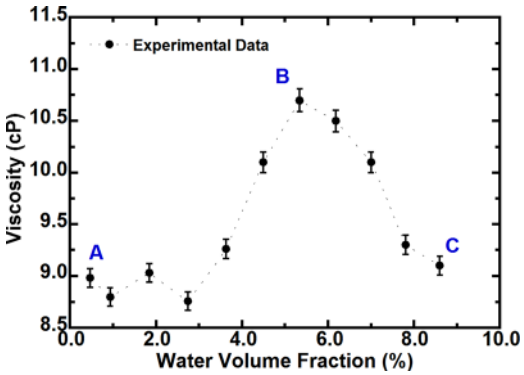

Fig. 4 Dynamic viscosity of water-in-PAO nanoemulsion fluids versus water volume fraction

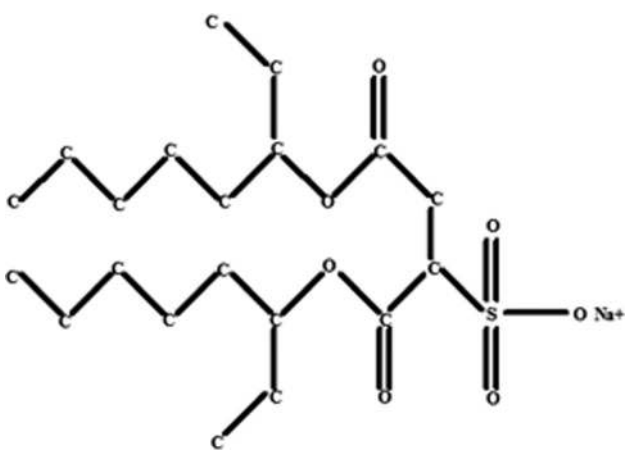

Fig. 5 Molecular structure of AOT-Na^+ surfactant

3 Experimental Results and Discussion

3.1 Thermal Conductivity of Water-in-PAO Nanoemulsion Fluids. Figure 3 shows the measured thermal conductivity in the water-in-PAO nanoemulsion fluids with water volume fraction from 0.47 vol. % to 8.6 vol. %. It can be seen that, the thermal conductivity increases approximately linearly with water volume fraction. A maximum increase in 16% is observed at water volume concentration 8.6 vol. %. This trend can be explained by the classic Maxwell equation [5,56–58]

$$\frac{k_{\text{eff}}}{k_0} = \frac{k_p + 2k_0 + 2\phi(k_p - k_0)}{k_p + 2k_0 - \phi(k_p - k_0)} \tag{2}$$

where k_0 is the thermal conductivity of the base fluid, k_p is the thermal conductivity of the particles, and ϕ is the particle volume fraction. Water has a thermal conductivity of 6 W/(m K), about four times larger than that of PAO. No anomalous enhancement of thermal conductivity is observed in the water-in-PAO nanoemulsion fluids tested in this study.

3.2 Dynamic Viscosity of Water-in-PAO Nanoemulsion Fluids. Figure 4 shows the measured dynamic viscosity of the water-in-PAO nanoemulsion fluids with water volume fraction from 0.47 vol. % to 8.6 vol. %. The test samples exhibit a shear-independent characteristic of Newtonian fluids for a spindle rotational speed from 10 to 30 rpm.

It can be seen in Fig. 5 that the viscosity first increases with water concentration, reaches a maximum at 5.3 vol. %, and then decreases. A similar trend is observed in other water-in-oil microemulsion systems [37,38]. The maximum in viscosity can be attributed to the attractive force between droplets within the nanoemulsion fluids. As the amount of water is increased, the surfactant AOT molecules become hydrated while releasing their counter ions into water. The molecular image of the surfactant AOT is shown in Fig. 5. The exchange of surfactants molecules and counterions between the droplets could become oppositely charged. The interdroplet attraction increases with water concentration till the hydration process is complete, which corresponds to the maximum viscosity observed in water-in-PAO nanoemulsion fluids [35,38,59].

3.3 Microstructure of Water-in-PAO Nanoemulsion Fluids. Figure 6 shows the processed SANS data for water-in-PAO nanoemulsion fluids with water concentration ranging from 1.8 vol. % to 10.3 vol. %. It can be seen in this figure that the neutron scattering curves can be categorized into three groups: 1) for water concentration of 1.8–4.5 vol. %, the curves level off when the scattering intensity q is less than 0.1 A^{-1}; 2) for water concentration of 5.3%–7.8 vol. %, those curves have a slightly downward sloping shape with increasing wave vector; 3) for water concentration of 8.6 vol. % and 10.3 vol. %, those curves shift to a more obvious ternary form.

The fitting of SANS data are processed using the IGOR PRO software under the protocol from NCNR NIST [13,47,53,60]. The hard-sphere model fits well for low water concentration curves (i.e., 1.8–4.5 vol. %), the nanodroplet radii are found to be 13.2 Å, 25.6 Å, and 96 Å for water loading 1.8 vol. %, 3.6 vol. %, and 4.5 vol. %, respectively. For higher water concentration (i.e., 7.8–10.3 vol. %), the hard-sphere model does not fit well especially for scattering q less than 0.1 A^{-1} region, which suggests

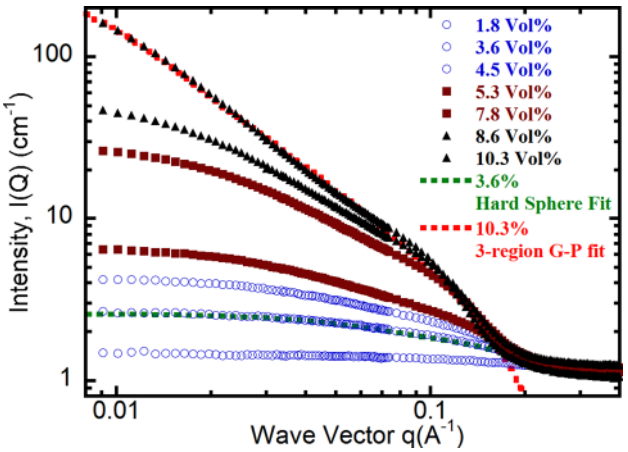

Fig. 6 Small-angle neutron scattering curves for water-in-PAO nanoemulsion fluids: water volume concentration from 1.8% to 10.3%. Three different symbols represent three different scattering curves.

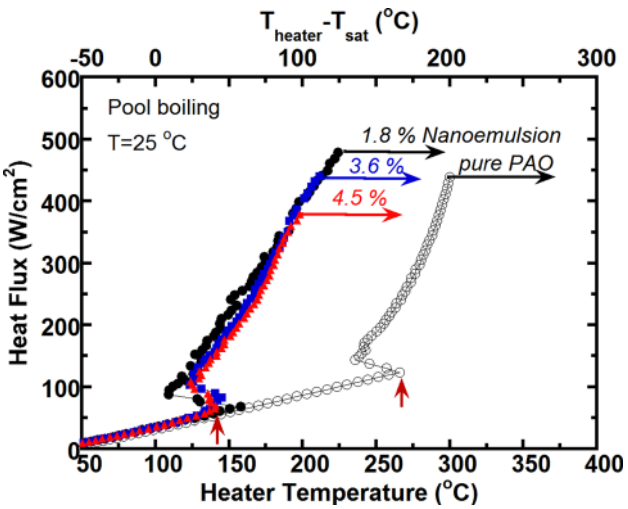

Fig. 7 Pool boiling curves for water-in-PAO nanoemulsion fluids: water volume fraction from 1.8% to 4.5%. The arrows in the figure represent where the burn out of wire occurs. $T_{saturation}$ is 100 °C for water at 1 atm.

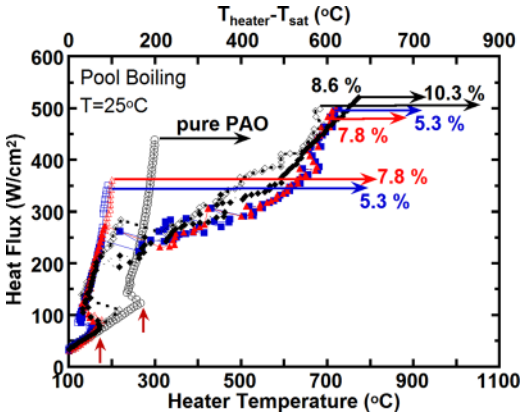

Fig. 8 Pool boiling curves for water-in-PAO nanoemulsion fluids: water volume concentration from 5.3% to 10.3%. The arrows in the figure represent where the burn out of wire occurs. $T_{saturation}$ is 100 °C for water at 1 atm.

that those nanodroplets are not simply spherical. The three-region Guinier-Porod empirical model is used to determine the nanodroplet geometry by fitting the SANS data.

In the three-region Guinier-Porod model, R_{g2} and R_{g1} are the radii of gyration for the short and overall sizes of the scattering object [60]. The fitted curves give $R_{g2} = 121$ Å, and $R_{g1} = 4.6$ Å for 10.3 vol. % sample. For 7.8 vol. % one, $R_{g2} = 47.4$ Å, and $R_{g1} = 5.2$ Å. These parameters suggest that the nanodroplets have a cylinder-like shape [60].

From the aforementioned analysis, it can be assessed that that the nanodroplet size and shape strongly depend on water concentration in water-PAO nanoemulsion fluids. The water nanodroplets change from sphere to elongated cylinder when the water concentration increases above 5.3 vol. % [35,61,62].

3.4 Pool Boiling of Water-in-PAO Nanoemulsion Fluids. Figure 7 shows the pool boiling curves for the nanoemulsion fluids with water volumetric concentration below 4.5 vol. %, and Fig. 8 is for concentration above 5.3 vol. %. As shown in Figs. 7 and 8, all tested water-in-PAO nanoemulsion fluids start to boil at around 170 °C. At low heat flux levels, single-phase natural convection appears to be the same for all water-in-PAO nanoemulsion fluids and for pure PAO. This indicates that without phase transitions, water nanodroplets have insignificant effect on the fluid heat transfer, which is consistent with the measured thermal conductivity and viscosity increase described in Secs. 3.1 and 3.2. At sufficiently large wall superheat (about 70 °C), nucleate boiling begins on the heater surface in these nanoemulsion fluids. After boiling incipience, the curves have a similar slope and appear to coincide for the water-in-PAO nanoemulsion fluids with different water concentrations [63,64]. It is observed that the CHF of these fluids decreases as water concentration increases in the measured water concentration range. For the transition region (5.3 vol. %–7.8 vol. %), the dependence of CHF on water concentration is very weak. It is generally accepted that CHF is accompanied by the formation of a vapor blanket and the dryout of a liquid sublayer between the blanket and the heated surface. The increase in water loading would facilitate the formation of water vapor layer between the PAO and the heated surface. Please note that the CHF of water-PAO nanoemulsion fluids is measured on a Pt wire 25 μm in diameter, so their values are expected to higher than those measured on a flat surface.

An interesting phenomenon observed in the experiment is that pool boiling of the water-in-PAO nanoemulsion fluids randomly varies between two different curves when the water concentration is larger than 5.3 vol. %, as shown in Fig. 8. In one set of boiling curves, the wire burnout occurs right after the critical heat flux is reached, without experiencing transition and film boiling. This set of curves is plotted with hollow symbols in Fig. 8. In another set of curves, the shift from nucleate boiling to transition boiling occurs at a lower heat flux, and the wire burns out in the film boiling regime. These curves are plotted in Fig. 8 with solid symbols. If the water content is increased above 8.6 vol. %, the wire burnout always occurs in the film boiling regime as shown in Fig. 8. It is also observed experimentally that the probability of the occurrence of the first type of boiling curves decreases with increasing water loading.

It is clear that the moderate change in thermal conductivity and viscosity in the water-PAO nanoemulsion fluids would not be responsible for the striking difference in pool boiling between the nanoemulsion fluids and the pure PAO. It is observed that water nanodroplets change from sphere to elongated cylinder as the water concentration increases over 5.3 vol. %. In this transition region, pool boiling of those nanoemulsion fluids varies between two curves.

No satisfactory explanation to this observed structure-property relation is currently available since the mechanisms of nanoemulsion boiling are little known.

4 Conclusion

In summary, thermophysical properties, microstructure, and pool boiling characteristics have been measured have been measured in the water-in-PAO nanoemulsion fluids with different water concentrations. Water-in-PAO nanoemulsion fluids are formed via self-assembly with AOT and are thermodynamically stable. The thermal conductivity increase is rather moderate in these fluids, for example, a 16% increase for 8.6 vol. % sample, which can be explained by the classical Maxwell model. The dynamic viscosity exhibits a maximum value of 10.7 cP at a water volume concentration around 5.3%. It is also found that the pool boiling characteristics are highly dependent upon water volumetric concentration. The pool boiling of nanoemulsion fluids randomly follows two different curves when the water concentration is in the range between 5.3 vol. % and 7.8 vol. %. In this transition region, water nanodroplets change from sphere to elongated cylinder shape and the interdroplet attraction reaches maximum due to hydrated surfactant molecules AOT.

Acknowledgment

This study is financially supported by National Science Foundation (CBET-0730963). The SANS measurements performed at the NIST-CNR are supported in part by the National Science Foundation under Agreement No. DMR-0944772.

The identification of commercial products does not imply endorsement by the National Institute of Standards and Technology nor does it imply that these are the best for the purpose.

Nomenclature

I = scattering intensity, cm^{-1}
k = thermal conductivity, W/(mK)
q = wave vector, A^{-1}
R = radii of gyration, A
S = dimensionality parameter
T = temperature, K

Greek Symbols

π = mathematical constant
θ = scattering angle
ϕ = volume fraction
λ = wavelength of the incident neutrons
δ = uncertainty

Subscripts

0 = base fluid
1 = parameter 1
2 = parameter 2
eff = Maxwell prediction
g1 = short size
g2 = overall size
p = particle
PAO = polyalphaolefin oil

References

[1] Eastman, L. J., Choi, S. U. S., Li, S., and Thompson, L. J., 1997, "Enhanced Thermal Conductivity Through Development of Nanofluids," Nanocryst. Nanocomp. Mater. II, **12**, pp. 457–468.
[2] Eastman, J. A., Choi, S. U. S., Li, S., Yu, W., and Thompson, L. J., 2001, "Anomalously Increased Effective Thermal Conductivities of Ethylene Glycol-Based Nanofluids Containing Copper Nanoparticles," Appl. Phys. Lett., **78**(6), pp. 718–720.
[3] Choi, S. U. S., Zhang, Z. G., Yu, W., Lockwood, F. E., and Grulke, E. A., 2001, "Anomalous Thermal Conductivity Enhancement in Nanotube Suspensions," Appl. Phys. Lett., **79**(14), pp. 2252–2254.
[4] You, S. M., Kim, J. H., and Kim, K. H., 2003, "Effect of Nanoparticles on Critical Heat Flux of Water in Pool Boiling Heat Transfer," Appl. Phys. Lett., **83**(16), pp. 3374–3376.
[5] Wen, D. S., and Ding, Y. L., 2004, "Effective Thermal Conductivity of Aqueous Suspensions of Carbon Nanotubes (Carbon Nanotubes Nanofluids)," J. Thermophys. Heat Transfer, **18**(4), pp. 481–485.
[6] Li, C. H., and Peterson, G. P., 2006, "Experimental Investigation of Temperature and Volume Fraction Variations on the Effective Thermal Conductivity of Nanoparticle Suspensions (Nanofluids)," J. Appl. Phys., **99**(8), p. 084314.
[7] Prasher, R., Evans, W., Meakin, P., Fish, J., Phelan, P., and Keblinski, P., 2006, "Effect of Aggregation on Thermal Conduction in Colloidal Nanofluids," Appl. Phys. Lett., **89**(14), p. 143119.
[8] Yang, B., and Han, Z. H., 2006, "Thermal Conductivity Enhancement in Water-in-FC72 Nanoemulsion Fluids," Appl. Phys. Lett., **88**(26), p. 261914.
[9] Yang, Y., Grulke, E. A., Zhang, Z. G., and Wu, G., 2006, "Thermal and Rheological Properties of Carbon Nanotube-in-Oil Dispersions," J. Appl. Phys., **99**(11), p. 114307.
[10] Yang, B., and Han, Z. H., 2006, "Temperature-Dependent Thermal Conductivity of Nanorod-Based Nanofluids," Appl. Phys. Lett., **89**(8), p. 083111.
[11] Han, Z. H., and Yang, B., 2008, "Thermophysical Characteristics of Water-in-FC72 Nanoemulsion Fluids," Appl. Phys. Lett., **92**(1), p. 013118.
[12] Xu, J. J., Wu, C. W., and Yang, B., 2010, "Thermal- and Phase-Change Characteristics of Self-Assembled Ethanol/Polyalphaolefin Nanoemulsion Fluids," J. Thermophys. Heat Transfer, **24**(1), pp. 208–211.
[13] Xu, J., Yang, B., and Hammouda, B., 2011, "Thermal Conductivity and Viscosity of Self-Assembled Alcohol/Polyalphaolefin Nanoemulsion Fluids," Nanoscale Res. Lett., **6**, pp. 274–280.
[14] Wu, C., Cho, T. J., Xu, J., Lee, D., Yang, B., and Zachariah, M. R., 2010, "Effect of Nanoparticle Clustering on the Effective Thermal Conductivity of Concentrated Silica Colloids," Phys. Rev. E, **81**(1), p. 011406.
[15] Xu, J., and Zhang, Y., 2009, "Analysis of Heat Transfer During Liquid-Vapor Pulsating Flow in a U-Shaped Miniature Channel," J. Enhanced Heat Transfer, **16**(4), pp. 367–385.
[16] Xu, J., Zhang, Y., and Ma, H., 2009, "Effect of Internal Wick Structure on Liquid-Vapor Oscillatory Flow and Heat Transfer in an Oscillating Heat Pipe," ASME J. Heat Transfer, **131**(12), p. 121012.
[17] Bergles, A. E., 1969, "Influence of Heated-Surface Vibration on Pool Boiling," ASME J. Heat Transfer, **91**(1), pp. 152–154.
[18] Bradfiel,W. S., 1967, "On Effect of Subcooling on Wall Superheat in Pool Boiling," ASME J. Heat Transfer, **89**(3), pp. 269–270.
[19] Bulanov, N. V., Skripov, V. P., and Khmylnin, V. A., 1984, "Heat Transfer to Emulsion With Superheating of Its Disperse Phase," J. Eng. Phys., pp. 1–3.
[20] Bulanov, N. V., Skripov, V. P., and Khmylnin, V. A., 1993, "Heat Transfer to Emulsion With a Low-Boiling Disperse Phase," Heat Transfer Res., pp. 786–789.
[21] Bulanov, N. V., 2001, "An Analysis of the Heat Flux Density Under Conditions of Boiling Internal Phase of Emulsion," High Temp., **39**(3), pp. 462–469.
[22] Bulanov, N. V., and Gasanov, B. M., 2005, "Experimental Setup for Studying the Chain Activation of Low-Temperature Boiling Sites in Superheated Liquid Droplets," Colloid J., **67**(5), pp. 531–536.
[23] Bulanov, N. V., Gasanov, B. M., and Turchaninova, E. A., 2006, "Results of Experimental Investigation of Heat Transfer With Emulsions With Low-Boiling Disperse Phase," High Temp., **44**(2), pp. 267–282.
[24] Bulanov, N. V., and Gasanov, B. M., 2008, "Peculiarities of Boiling of Emulsions With a Low-Boiling Disperse Phase," Int. J. Heat Mass Transfer, **51**(7–8), pp. 1628–1632.
[25] Henry, C. D., and Kim, J. H., 2004, "A Study of the Effects of Heater Size, Subcooling, and Gravity Level on Pool Boiling Heat Transfer," Int. J. Heat Fluid Flow, **25**(2), pp. 262–273.
[26] Kim, J. B., Oh, B. D., and Kim, M. H., 2006, "Experimental Study of Pool Temperature Effects on Nucleate Pool Boiling," Int. J. Multiphase Flow, **32**(2), pp. 208–231.
[27] Kim, S. J., Bang, I. C., Buongiorno, J., and Hu, L. W., 2007, "Surface Wettability Change During Pool Boiling of Nanofluids and its Effect on Critical Heat Flux," Int. J. Heat Mass Transfer, **50**(19–20), pp. 4105–4116.
[28] Kim, B. H., Beskok, A., and Cagin, T., 2008, "Molecular Dynamics Simulations of Thermal Resistance at the Liquid-Solid Interface," J. Chem. Phys., **129**(17), p. 174701.
[29] Rosele, M. L., 2010, "Boiling of Dilute Emulsions," Ph.D. dissertation, University of Minnesota, Twin Cities, MN.
[30] Roesle, M. L., and Kulacki, F. A., 2010, "Boiling of Dilute Emulsions-Toward a New Modeling Framework," Ind. Eng. Chem. Res., **49**(11), pp. 5188–5196.
[31] Shai, I., and Rohsenow, W. M., 1969, "Mechanism of and Stability Criterion for Nucleate Pool Boiling of Sodium," ASME J. Heat Transfer, **91**(3), pp. 315–328.
[32] Shepherd, J. E., and Sturtevant, B., 1982, "Rapid Evaporation at the Superheat Limit," J. Fluid Mech., **121**, pp. 379–402.
[33] Kandlikar, S. G., Shoji, M., and Dhir, V. K., 1999, *Handbook of Phase Change:Boiling and Condensation*, Taylor & Francis, London.
[34] Kandlikar, S. G., 2001, "A Theoretical Model to Predict Pool Boiling CHF Incorporating Effects of Contact Angle and Orientation," ASME J. Heat Transfer, **123**(6), pp. 1071–1079.
[35] Kumar, P., and Mittal, K. L., 1999, *Handbook of Microemulsion Science and Technology*, Marcel Dekker, New York.
[36] Moulik, S. P., and Ray, S., 1994, "Thermodynamics of Clustering of Droplets in Water/AOT/Heptane Microemulsion," Pure Appl. Chem., **66**(3), pp. 521–525.
[37] Bergenholtz, J., Romagnoli, A. A., and Wagner, N. J., 1995, "Viscosity, Microstructure, and Interparticle Potential of AOT/H_2O/N-Decane Inverse Microemulsions," Langmuir, **11**(5), pp. 1559–1570.

[38] Batra, U., Russel, W. B., and Huang, J. S., 1999, "Viscosity Anomaly and Charge Fluctuations in Dilute AOT Microemulsions With X < 20," Langmuir, **15**(11), pp. 3718–3725.
[39] Hirai, M., Kawai-Hirai, R., Sanada, M., Iwase, H., and Mitsuya, S., 1999, "Characteristics of AOT Microemulsion Structure Depending on a Polar Solvents," J. Phys. Chem. B, **103**(44), pp. 9658–9662.
[40] Hirai, M., Hirai, R. K., Iwase, H., Arai, S., Mitsuya, S., Takeda, T., Seto, H., and Nagao, M., 1999, "Dynamics of w/o AOT Microemulsions Studied by Neutron Spin Echo," J. Phys. Chem. Solids, **60**(8–9), pp. 1359–1361.
[41] Lawrence, M. J., and Warisnoicharoen, W., 2006, "Recent Advances in Microemulsions as Drug Delivery Vehicles," *Nanoparticles as Drug Carriers*, Imperial College Press, London.
[42] Tyndall, J., 1868, "On the Blue Colour of the Sky, the Polarization of Sky-Light, and on the Polarization of Light by Cloudy Matter Generally," Proc. R. Soc. London, **17**, pp. 223–233.
[43] He, G. S., Qin, H.-Y., and Zheng, Q., 2009, "Rayleigh, Mie, and Tyndall Scatterings of Polystyrene Microspheres in Water: Wavelength, Size, and Angle Dependences," J. Appl. Phys., **105**(2), p. 023110.
[44] Yang, B., Liu, W. L., Liu, J. L., Wang, K. L., and Chen, G., 2002, "Measurements of Anisotropic Thermoelectric Properties in Superlattices," Appl. Phys. Lett., **81**(19), pp. 3588–3590.
[45] Cahill, D. G., 1990, "Thermal-Conductivity Measurement From 30-K to 750-K—The 3-Omega Method," Rev. Sci. Instrum., **61**(2), pp. 802–808.
[46] Chevron Phillips Chemical LP, 2002, *Synfluid PAO Databook*, The Woodlands, TX.
[47] Hammouda, B., 2010, "SANS From Polymers-Review of the Recent Literature," Polym. Rev., **50**(1), pp. 14–39.
[48] Liu, J. C., Li, G. Z., and Han, B. X., 2001, "Characteristics of AOT Microemulsion Structure: A Small Angle X-Ray Scattering Study," Chin. Chem. Lett., **12**(11), pp. 1023–1026.
[49] Howe, A. M., Toprakcioglu, C., Dore, J. C., and Robinson, B. H., 1986, "Small-Angle Neutron-Scattering Studies of Microemulsions Stabilized by Aerosol-OT 3. The Effect of Additives on Phase-Stability and Droplet Structure," J. Chem. Soc., Faraday Trans. 1, **82**, pp. 2411–2422.
[50] Bisal, S., Bhattacharya, P. K., and Moulik, S. P., 1990, "Conductivity Study of Microemulsions—dependence of Structural Behavior of Water Oil Systems on Surfactant, Cosurfactant, Oil, and Temperature," J. Phys. Chem., **94**(1), pp. 350–355.
[51] Nagao, M., Seto, H., Shibayama, M., and Yamada, N. L., 2003, "Small-Angle Neutron Scattering Study of Droplet Density Dependence of the Water-in-Oil Droplet Structure in a Ternary Microemulsion," J. Appl. Crystallogr., **36**, pp. 602–606.
[52] Kotlarchyk, M., Chen, S. H., and Huang, J. S., 1982, "Temperature-Dependence of Size and Polydispersity in a 3-Component Micro-Emulsion by Small-Angle Neutron-Scattering," J. Phys. Chem., **86**(17), pp. 3273–3276.
[53] Hammouda, B., Krueger, S., and Glinka, C. J., 1993, "Small-Angle Neutron-Scattering at the National-Institute-of-Standards-and-Technology," J. Res. Natl. Inst. Stand. Technol., **98**(1), pp. 31–46.
[54] Gradzielski, M., and Langevin, D., 1996, "Small-Angle Neutron Scattering Experiments on Microemulsion Droplets: Relation to the Bending Elasticity of the Amphiphilic Film," J. Mol. Struct., **383**(1–3), pp. 145–156.
[55] Marszalek, J., Pojman, J. A., and Page, K. A., 2008, "Neutron Scattering Study of the Structural Change Induced by Photopolymerization of AOT/D(2)O/Dodecyl Acrylate Inverse Microemulsions," Langmuir, **24**(23), pp. 13694–13700.
[56] Buongiorno, J., Venerus, D. C., Prabhat, N., McKrell, T., Townsend, J., Christianson, R., Tolmachev, Y. V., Keblinski, P., Hu, L.-W., Alvarado, J. L., Bang, I. C., Bishnoi, S. W., Bonetti, M., Botz, F., Cecere, A., Chang, Y., Chen, G., Chen, H., Chung, S. J., Chyu, M. K., Das, S. K., Di Paola, R., Ding, Y., Dubois, F., Dzido, G., Eapen, J., Escher, W., Funfschilling, D., Galand, Q., Gao, J., Gharagozloo, P. E., Goodson, K. E., Gutierrez, J. G., Hong, H., Horton, M., Hwang, K. S., Iorio, C. S., Jang, S. P., Jarzebski, A. B., Jiang, Y., Jin, L., Kabelac, S., Kamath, A., Kedzierski, M. A., Kieng, L. G., Kim, C., Kim, J.-H., Kim, S., Lee, S. H., Leong, K. C., Manna, I., Michel, B., Ni, R., Patel, H. E., Philip, J., Poulikakos, D., Reynaud, C., Savino, R., Singh, P. K., Song, P., Sundararajan, T., Timofeeva, E., Tritcak, T., Turanov, A. N., Van Vaerenbergh, S., Wen, D., Witharana, S., Yang, C., Yeh, W.-H., Zhao, X.-Z., and Zhou, S.-Q., 2009, "A Benchmark Study on the Thermal Conductivity of Nanofluids," J. Appl. Phys., **106**(9), p. 094312.
[57] Maxwell, J. C., 1904, "*A Treatise on Electricity and Magnetism*," Oxford University Press, Cambridge, UK.
[58] Nan, C. W., Birringer, R., Clarke, D. R., and Gleiter, H., 1997, "Effective Thermal Conductivity of Particulate Composites With Interfacial Thermal Resistance," J. Appl. Phys., **81**(10), pp. 6692–6699.
[59] Alexandridis, P., Holzwarth, J. F., and Hatton, T. A., 1995, "Thermodynamics of Droplet Clustering in Percolating AOT Water-in-Oil Microemulsions," J. Phys. Chem., **99**(20), pp. 8222–8232.
[60] Hammouda, B., 2010, "A New Guinier-Porod Model," J. Appl. Crystallogr., **43**, pp. 716–719.
[61] Blokhuis, E. M., and Sager, W. F. C., 2001, "Sphere to Cylinder Transition in a Single Phase Microemulsion System: A Theoretical Investigation," J. Chem. Phys., **115**(2), pp. 1073–1085.
[62] Langevin, D., 1992, "Micelles and Microemulsion," Annu. Rev. Phys. Chem., **43**, pp. 341–369.
[63] Hodgson, A. S., 1969, "hysteresis Effects in Surface Boiling of Water," ASME J. Heat Transfer, **91**(1), pp. 160–162.
[64] Celata, G. P., Cumo, M., and Setaro, T., 1992, "hysteresis Phenomena in Subcooled Flow Boiling of Well-Wetting Fluids," Exp. Heat Transfer, **5**(4), pp. 253–275.